


Diallyl Disulfide Attenuates Ionizing Radiation-Induced Migration and Invasion by Suppressing Nrf2 Signaling in Non-small-Cell Lung Cancer

Dose-Response:
An International Journal
July-September 2021:1-11
© The Author(s) 2021
Article reuse guidelines:
sagepub.com/journals-permissions
DOI: 10.1177/15593258211033114
journals.sagepub.com/home/dos


Shuai Xu^{1,2,*}, Hefa Huang^{3,*}, Deping Tang⁴, Mengjie Xing⁴,
Qiuyue Zhao^{2,5}, Jianping Li¹, Jing Si², Lu Gan²,
Aihong Mao^{2,6}, and Hong Zhang²

Abstract

Non-small-cell lung cancer (NSCLC) is the leading cause of cancer-associated deaths. Radiotherapy remains the primary treatment method for NSCLC. Despite great advances in radiotherapy techniques and modalities, recurrence and resistance still limit therapeutic success, even low-dose ionizing radiation (IR) can induce the migration and invasion. Diallyl disulfide (DADS), a bioactive component extracted from garlic, exhibits a wide spectrum of biological activities including antitumor effects. However, the effect of DADS on IR-induced migration and invasion remains unclear. The present study reported that IR significantly promoted the migration and invasion of A549 cells. Pretreatment with 40 μ M DADS enhanced the radiosensitivity of A549 cells and attenuated IR-induced migration and invasion. In addition, 40 μ M DADS inhibited migration-related protein matrix metalloproteinase-2 and 9 (MMP-2/9) expression and suppressed IR-aggravated EMT by the upregulation of the epithelial marker, E-cadherin, and downregulation of the mesenchymal marker, N-cadherin, in A549 cells. Furthermore, DADS was found to inhibit the activation of Nrf2 signaling. Based on our previous results that knockdown of Nrf2 by siRNA suppressed IR-induced migration and invasion in A549 cells, we speculated that DADS attenuated IR-induced migration and invasion by suppressing the activation of Nrf2 signaling in A549 cells.

Keywords

diallyl disulfide, ionizing radiation, migration, invasion, Nrf2, non-small-cell lung cancer

Introduction

Lung cancer is one of the most commonly occurring malignant tumors in humans. It is a leading cause of cancer-associated death, and 2 206 771 new cases and 1 796 144 deaths were reported worldwide in 2020.¹ Non-small-cell lung cancer (NSCLC) is the most common type of lung cancer, accounting for 85% of diagnosed cases. According to the estimates of the World Health Organization (WHO), 1.8 million patients per year are diagnosed with NSCLC.² Radiotherapy remains to be the primary treatment method for NSCLC either alone or in combination.^{3,4} Despite the considerable progress in radiotherapy technology, there are several limitations that affect the

¹Zhaoqing Medical College, Zhaoqing, China

²Institute of Modern Physics, Chinese Academy of Sciences, Lanzhou, China

³School of Nuclear Science and Technology, Lanzhou University, Lanzhou, China

⁴School of Biological & Pharmaceutical Engineering, Lanzhou Jiaotong University, Lanzhou, China

⁵Human Resources Office, Sichuan University, Chengdu, China

⁶Gansu Provincial Academic Institute for Medical Research, Lanzhou 730050, China

Received 1 March 2021; received revised 27 June 2021; accepted 28 June 2021

*Shuai Xu and Hefa Huang contributed to this work.

Corresponding Authors:

Aihong Mao, Gansu Provincial Academic Institute for Medical Research, Lanzhou 730050, China.

Email: maoaih@impcas.ac.cn

Hong Zhang, Department of Heavy Ion Radiation Medicine, Institute of Modern Physics, Chinese Academy of Sciences, Lanzhou 730000, China.

Email: zhangh@impcas.ac.cn



Creative Commons Non Commercial CC BY-NC: This article is distributed under the terms of the Creative Commons Attribution-NonCommercial 4.0 License (<https://creativecommons.org/licenses/by-nc/4.0/>) which permits non-commercial use, reproduction and distribution of the work without further permission provided the original work is attributed as specified on the SAGE

and Open Access pages (<https://us.sagepub.com/en-us/nam/open-access-at-sage>).

outcome of radiotherapy. Radioresistance and distant metastasis are major challenges for the clinical treatment of NSCLC.⁵ An increasing number of studies point out that most NSCLC patients are already in an advanced or metastatic stage at the time of initial diagnosis, resulting in a lower 5-year survival rate.⁶ Considering the high mortality and incidence rates, it is urgent to identify novel treatment strategies to block cancer metastasis and improve the prognosis of NSCLC patients.

Recently, diallyl disulfide (DADS), an oil-soluble compound extracted from garlic (*Allium sativum* L.), has been reported to exhibit antitumor by inhibiting cell cycle arrest, inducing apoptosis, and reducing invasion and metastasis.⁷⁻¹² In NSCLC, early research showed that DADS was effective in reducing the anti-proliferative gene and inducing apoptosis in both H460 and H1299 cells.¹³ Recently, Hui et al. demonstrated that DADS-induced apoptosis in H1299 cells, at least partly, via G2/M-phase block of the cell cycle, related to an increase in MAPK phosphorylation.¹⁴ Notably, NSCLC-related mortality is associated with the development of the metastatic potential of the primary tumor.¹⁵ Moreover, increasing literature suggests at higher mRNA expression of epithelial mesenchymal transition (EMT) markers in NSCLC specimens, indicating the involvement of EMT in NSCLC metastasis.¹⁶ Interestingly, Das B et al. recently reported that DADS could reduce migration of A549 cells via suppressing the canonical Wnt signaling pathway and reverse the fibronectin (FN)-induced EMT.¹⁰ In this study, the authors selected the A549 cell line, the most aggressive and commonly used model for NSCLC, to investigate the role of DADS in the modulation of FN-induced EMT.¹⁷ The function of FN in regulating normal cell adhesion and migration has been well documented.¹⁸ Additionally, Li et al have shown that FN-induced EMT in MCF-7 cells via the activation of calpain.¹⁹ Due to when tumor cells are exposed to low doses of X-rays, their proliferation ability is significantly suppressed, while migration and invasion capabilities are significantly enhanced.²⁰⁻²² Although DADS were previously reported to enhance radiation-induced apoptosis and suppress cancer cell proliferation in cervical cancer cells,²³ the effect of DADS on radiation-induced migration and invasion of NSCLC and its molecular mechanisms are currently unknown.

Nrf2 (nuclear factor erythroid 2-related factor 2, Nrf2) is a redox-sensitive transcription factor.²⁴ Besides mediating adaptive response by regulating the expression of intracellular antioxidant and detoxification enzymes, Nrf2 plays a dual role in tumor initiation and progression. On one hand, Nrf2-deficient mice showed increased susceptibility to carcinogenesis and metastasis in multiple mouse models.²⁵ On the other hand, aberrant Nrf2 activation enhances tumorigenic potential by actively promoting cancer cell proliferation, angiogenesis, and metastasis.²⁴ It has been demonstrated that constitutive activation of Nrf2 in lung cancer cells promotes tumorigenicity, and knockdown of Nrf2 expression inhibits tumor growth.^{26,27} Activation of Nrf2

accelerates tumor metastasis and invasion,^{28,29} and loss of Nrf2 reverses propofol-induced invasion.³⁰ In response to ionizing radiation, several studies suggested Nrf2 was activated, resulting in radioresistance, even migration and invasion of cancer cells.^{31,32} In lung cancers, Nrf2 gain-of-function mutations often occur, and higher intratumoral levels of Nrf2 are associated with poor clinical outcomes.³³⁻³⁶ However, currently, little evidence is available on the effect of DADS on Nrf2 expression in response to radiation. Whether and how DADS influences IR-induced migration and invasion in NSCLC is still unknown.

Previously, we found that the synergistic interaction between Nrf2 and Notch1 signaling plays a critical role in IR-induced migration and invasion in A549 cells.³⁷ Therefore, in the present study, we hypothesized that radiation enhanced the invasion and migration of NSCLC by activating Nrf2 signaling, and DADS could inhibit the activation of Nrf2 signaling, leading to IR-induced migration of NSCLC was attenuated. The study aimed to observe the effect of DADS on IR-induced migration and invasion in A549 cells and to identify a promising candidate to overcome the migration and invasion of NSCLC radiotherapy.

Materials and Methods

Reagents

Diallyl disulfide was provided by Sigma-Aldrich. Primary antibodies against Nrf2, HO-1, NQO-1, MMP-2, MMP-9, E-cadherin, N-cadherin, and β -actin were purchased from Abcam (Cambridge, MA, USA).

Cell Culture and Irradiation Treatment

A549 cells were grown in RPMI-1640 (Gibco Life Technologies, Carlsbad, CA, USA) medium supplemented with 10% (v/v) fetal bovine serum (Hyclone, GE Healthcare Life Sciences, Logan, USA) and incubated at 37°C in a humidified 5% CO₂ atmosphere.

The A549 cells were exposed to X-ray irradiation at 22°C. X-rays were generated using an RX-650 instrument (Faxitron Bioptics, LLC, USA) at 100 kV/s. The dose rate was .924 Gy/min.

Cell Viability and Proliferation Assays

A549 cells (2×10^3 cells/well) were seeded in 96-well plates and incubated at 37°C with 5% CO₂ in a humidified environment. After 24 h, the cells were pretreated with various concentrations of DADS (0-80 μ M) and/or IR (4 Gy X-rays). The MTS assay was performed using CellTiter 96[®] Aqueous One Solution Cell Proliferation Assay (Promega Corp., Madison, WI, USA). Proliferation assays were performed using the cell counting Kit-8 (CCK-8) kit (Dojindo, Kumamoto, Japan)

Colony Formation Assay

A549 cells with 80% confluence were exposed to 0, 1, 2, 4, 6, and 8 Gy X-ray irradiation at room temperature. The irradiated cells were trypsinized and 2×10^3 cells were seeded in 60 mm dishes. The cells were incubated under a static condition for 13 days. The colonies were fixed with 100% methanol for 15 min and stained with .5% crystal violet (Sigma-Aldrich) for 30 min at room temperature. Only colonies containing more than 50 cells were counted for each treatment group. Cell susceptibility was described as the inverse value of survival for a given dose of exposure from the α and β parameters for each survival dataset. The α and β parameters were obtained from survival data by curve fitting using $SF = \exp(-\alpha D - \beta D^2)$, where SF is the survival fraction and D is the irradiation dose.

Migration and Invasion Assay

For migration assays, DADS and/or IR-treated A549 cells were serum-starved for 24 h for cell cycle synchronization, and the confluent cell monolayer (seeded in 35 mm culture dishes) was scraped with a 200 μ L sterile pipette tip to create a wound artificially. The wound healing process was observed at the indicated time points and photographed.

For invasion assays, 1×10^6 cells were plated in the top chamber with Matrigel-coated membrane (24-well insert; pore size, 8 μ m; BD Biosciences) in 400 μ L serum-free medium, and 600 μ L complete medium was added to the lower chamber. The cells were incubated for 24 h and cells that did not invade through the pores were removed using a cotton swab. Cells on the lower surface of the membrane were fixed with 4% paraformaldehyde solution and stained with Giemsa. Images of the invaded cells were obtained using a microscope (Carl Zeiss, Germany).

Reverse Transcription-Polymerase Chain Reaction

After the cells were treated with DADS and/or IR, total RNA was extracted using TRIzol reagent (Takara Biotech Co., Ltd.). Reverse transcription was performed using a PrimeScript RT Master Mix (Takara Biotech Co., Ltd.) in a total volume of 20 μ L. Quantitative PCR was conducted with the SYBR Premix Ex Taq II kit (Takara Biotech Co., Ltd.) with specific primers (Table 1). Relative expression of the target mRNA was evaluated with the levels of β -actin using the $2^{-\Delta\Delta C_t}$ method.

Enzyme-Linked Immunosorbent Assay

Culture supernatants of treated or untreated A549 cells were centrifuged at 5000 r/min for 5 min. The activities of MMP-2 and MMP-9 in the supernatants were measured using an ELISA kit (Excell Bio. China), according to the manufacturer's instructions. The absorbance was detected using a

Table 1. Primer sequences for specific genes and reference genes.

Gene	Sequence
Nrf2	F 5'-AGCCCAGCACATCCAGTCA-3' R 5'-TGCATGCAGTCATCAAAGTACAAAG-3'
HO-1	F 5'-CATGACACCAAGGACCAGAG-3' R 5'-AGTGTAAGGACCCATCGGAG-3'
NQO-1	F 5'-TTCTCTGGCCGATTCAGAG-3' R 5'-GGCTGCTTGGAGCAAAATAG-3'
β -actin	F 5'-ACACTGTGCCCATCTACGAGGGG-3' R 5'-ATGATGGAGTTGAAGGTAGTTTCGTGGAT-3'

Abbreviations: F, forward primer; R, reverse primer.

microplate reader (Tecan Infinite M200, Switzerland) at 450 nm within 2 h after adding the stop solution. The concentrations of MMP2 and MMP-9 were calculated using the standard curve.

Western Blot Analysis

A549 cells treated with DADS and/or IR were lysed using RIPA buffer containing 1% PMSF (Beyotime, Haimen, China) on ice. The concentration of total protein was determined using bicinchoninic acid protein assay (Thermo, USA). Thereafter, 20 μ g of total protein was loaded onto 10% SDS-PAGE and then transferred to a PVDF membrane (Millipore, IPVH00010), blocked with .05% Tween and 5% BSA (bovine serum albumin, BSA) (BBI Life Sciences Corporation, Canada) in Tris-buffered saline for 2 h. Followed by incubation with primary antibodies: N-cadherin (ab18203), E-cadherin (ab1416), MMP-2 (ab92536), MMP-9 (ab76003), Nrf2 (ab62352), HO-1 (ab13248), NQO-1 (ab80588), and β -actin (AP0060) overnight at 4°C. The preparative membranes were reacted with appropriate secondary antibodies conjugated to HRP. The immunological complexes were visualized using electrochemiluminescence (Millipore, Darmstadt, Germany). The protein bands were detected using AI680 (Alpha Innotech Corporation) and quantified using Image Quant TL software (version 8.1; GE Healthcare Life Sciences).

Immunofluorescence Staining

Cells were cultured on coverslips and fixed in 4% paraformaldehyde for 20 min at room temperature. Cells were washed three times with PBS and incubated with .3% Triton X-100 for 10 min and blocked with PBS containing 5% BSA for 1 h. The cells were incubated with anti-E-cadherin and anti-N-cadherin antibodies overnight at 4°C washed three times with PBS, and stained with Alexa Fluor 647-conjugated (red) and Alexa Fluor 488-conjugated (green) secondary antibodies for 1 h. After two washes with PBS, the samples were incubated with DAPI (4', 6'-diamidino-2-phenylindole, DAPI; .5 mg/mL) (blue) for 5 min. All

images were scanned using a confocal fluorescence microscope (LSM700; Carl Zeiss).

Statistical Analysis

Results are presented as means \pm standard deviation (SD). Significant differences in means between two samples were analyzed using two-tailed Student's *t*-tests and two-way

ANOVA. Statistically significance was set at $P < .05$ was considered.

Results

Effect of DADS on Viability and Proliferation of A549 Cells

To determine the effect of DADS on the viability of A549 cells, the cells were treated with different concentrations

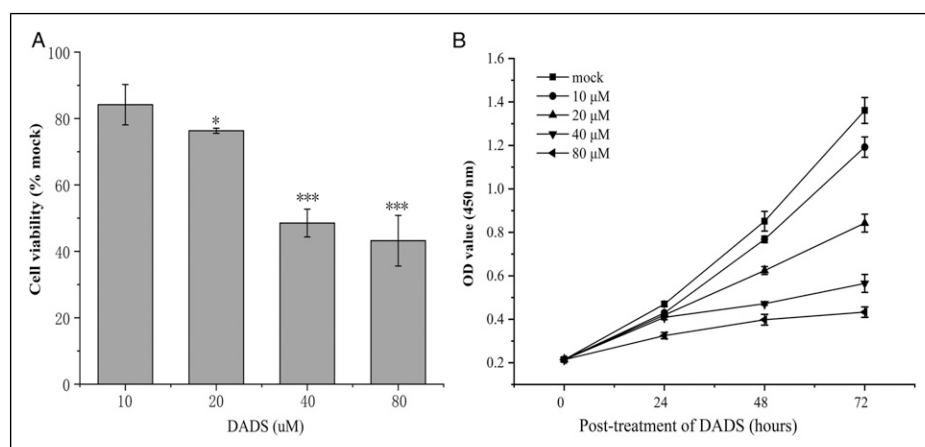


Figure 1. DADS inhibited the viability and proliferation of A549 cells. (A) A549 cells were treated with DADS at different concentrations (0–80 μ M) for 24 h and cell viability was detected by MTS assay. (B) A549 cells were treated with DADS at different concentrations (0–80 μ M) for 24, 48, and 72 h, and CCK-8 kit was used to analyze the proliferation. * $P < .05$, *** $P < .001$ vs mock group. DADS: diallyl disulfide.

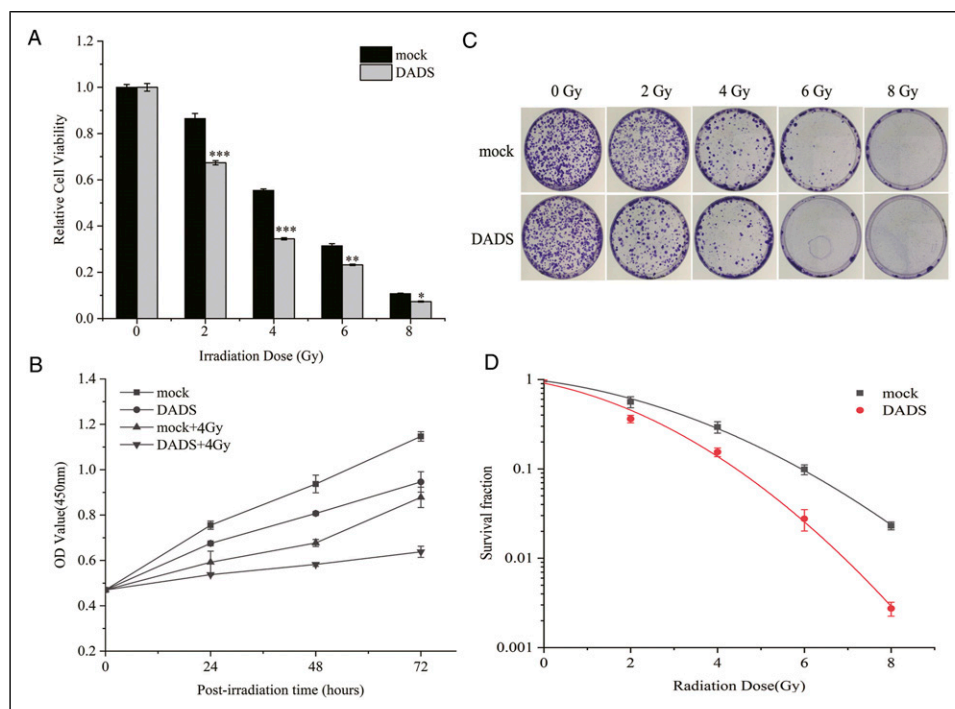


Figure 2. DADS enhanced the radiosensitivity of A549 cells. (A) The relative cell viability of A549 cells pretreated with 40 μ M DADS for 24 h before X-ray irradiation at different doses (0, 2, 4, 6, and 8 Gy). (B) Cell proliferation of A549 cells pretreated with 40 μ M of DADS and 4 Gy X-ray. (C) and (D) Clonogenicity was measured in A549 cells pretreating with 40 μ M DADS and/or indicated doses of X-ray irradiation. * $P < .05$, ** $P < .01$ and *** $P < .001$ vs mock group. DADS: diallyl disulfide.

(0–80 μM) of DADS for 24 h and the MTS assay was performed. The results revealed that DADS inhibited the cell viability in concentration-dependent manner compared to the mock (dimethylsulfoxide, DMSO) group (Figure 1A). After treatment with 40 μM DADS for 24 h, cell viability was significantly inhibited ($P < .001$). Cell proliferation of A549 cells was significantly inhibited after treatment with more than 40 μM DADS ($P < .01$) (Figure 1B). 40 μM of DADS was the effective concentration. Therefore, 40 μM concentration was selected for further experiments.

DADS Enhanced the Radiosensitivity of A549 Cells

The effect of DADS and IR on A549 cell viability was examined by treating the cells with 40 μM DADS for 24 h prior to exposure to different doses of X-rays. As shown in Figure 2A and B, pretreatment with 40 μM DADS promoted IR-induced viability decrease and proliferation inhibition. Furthermore, a colony forming assay showed that pretreatment with 40 μM DADS enhanced the radiosensitivity of A549 (Figure 2C and D).

DADS Attenuated IR-Induced Migration and Invasion of A549 Cells

To evaluate the effect of DADS on migration and invasion in IR-treated A549 cells, scratch, transwell and Matrigel invasion assays were performed. As shown in Figure 3A and B, the results revealed that IR significantly promoted the migration of A549 cells. After treatment with 40 μM DADS for 24 h prior to IR, they migrated ~20% slower than that of mock cells and ~62% slower than that of IR-treated cells. When these cells were treated with both DADS and IR, there was a 35% reduction in gap closure than that of IR-treated cells. Similarly, pretreatment of DADS attenuated IR-induced invasion of A549 cells (Figure 3C and D). These data suggested that 40 μM DADS effectively suppressed the migration and invasion of IR-treated A549 cells.

DADS Inhibited Migration-Related Protein Expression in A549 Cells

The efficacy of DADS in the suppression of IR-induced migration encouraged us to investigate the effect of DADS on the activities of MMP-2 and MMP-9 in IR-treated A549 cells. As the results of ELISA, assays showed that IR enhanced the activities of MMP-2 and MMP-9 but was efficiently counteracted by DADS (40 μM) pretreatment (Figure 4A and B). In addition, the results of western blotting also demonstrated that the levels of MMP-2 and MMP-9 were markedly increased in IR-treated A549 cells, while pretreatment with

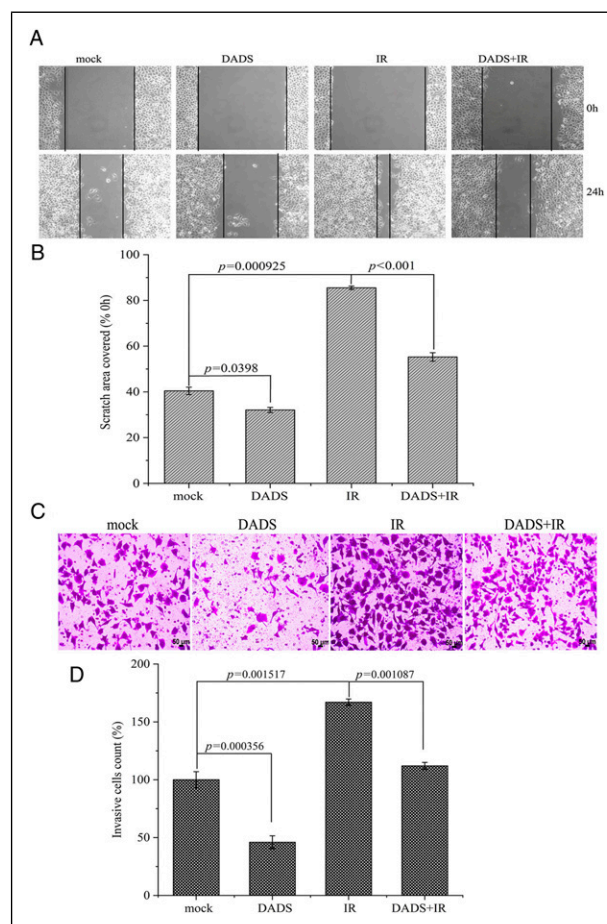


Figure 3. DADS attenuated IR-induced migration and invasion of A549 cells. (A) and (B) Representative images and quantitative analysis of cell migration based on wound healing assays (scale bar, 200 μm). (C) and (D) Representative images and quantitative analysis of cell invasion based on transwell assays (scale bar, 50 μm). DADS: diallyl disulfide.

40 μM DADS significantly decreased the levels of both MMP-2 and MMP-9 in IR-treated A549 cells (Figure 4C and D).

DADS Suppressed the Characteristic Markers of EMT in IR-Treated A549 Cells

The potency of DADS in the modulation of cell migration and invasion prompted us to examine whether DADS could reverse the process of EMT in IR-treated A549 cells. As shown in Figure 5, IR suppressed the epithelial marker, E-cadherin, when comparison with that of mock cells. Pretreatment with DADS (40 μM) increased the expression of E-cadherin. While, IR enhanced the mesenchymal marker, N-cadherin, and pretreatment with DADS (40 μM) significantly reduced the levels of N-cadherin. The results were evident from both immunocytochemistry (Figure 5A) and western blot (Figure 5B–D). These data suggest that 40 μM DADS confers intercellular

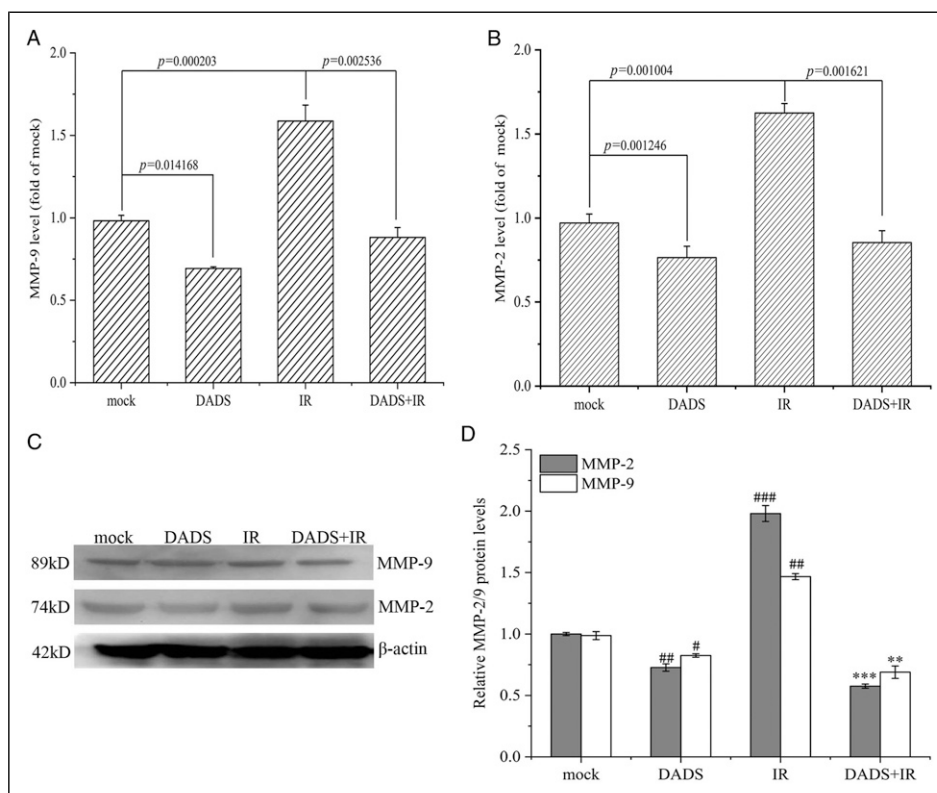


Figure 4. DADS inhibited IR-induced MMP-9 and MMP-2 protein expression in A549 cells. (A) and (B) A549 cells were treated with 40 μ M DADS or 4 Gy X-ray, an ELISA assay to analyse the MMP-9 and MMP-2 levels. (C) and (D) Western blotting was used to detect the levels of MMP-9 and MMP-2 protein. β -actin served as a control. Data are representative of at least three independent experiments. # $P < .05$, ## $P < .01$ and ### $P < .001$ vs mock group; ** $P < .01$ and *** $P < .001$ vs IR-treated group. DADS: diallyl disulfide.

junctions through the regulation of E-cadherin and N-cadherin protein expression.

DADS Inhibited IR-Induced Migration and Invasion Was Associated With the Suppression of Nrf2 Signaling Pathway

As shown in Figure 6A and B, the mRNA levels of Nrf2 were reduced after treated with 40 μ M DADS at 12 and 24 h (Figure 6A) and protein levels significantly decreased in A549 cells treated with different concentrations of DADS (Figure 6B). Furthermore, IR significantly increased mRNA and protein levels of Nrf2 and its target genes HO-1 and NQO1, whereas the mRNA and protein levels of Nrf2, HO-1 and NQO1 levels were reduced after cells were treated with 40 μ M DADS (Figure 6C and D). These results indicated that DADS attenuated IR-induced activation of the Nrf2 signaling pathway.

Discussion

Lung cancer is one of the most malignant tumors with the highest morbidity and mortality worldwide.³⁸ NSCLC, the most frequently occurring category of lung cancer, accounts

for approximately 85% of all cases.^{2,38} Tumor invasion and metastasis are the main factors responsible for NSCLC treatment failure.^{15,39} Despite great advances in radiotherapy techniques and modalities, recurrence and resistance still limit the therapeutic success. There is evidence that when tumor cells are exposed to low doses of X-rays, their viability and proliferation ability is significantly suppressed, while migration and invasion capabilities are significantly enhanced;²⁰⁻²² thus, seeking novel approaches or agents to reverse IR-induced tumor cell invasion and migration is the key to overcoming tumor recurrence and metastasis during radiotherapy for NSCLC.

Diallyl disulfide, a major organosulfur compound derived from garlic, were reported to exhibit various pharmacological properties such as antibacteria, antiangiogenesis, anticancer, and anticoagulation.⁹ Besides, DADS are also reported to induce cytotoxicity and induction of cell death in various human cancer cells.^{7,21,40} It has been indicated that DADS could suppress cell migration and the invasion in human triple negative breast cancer,⁷ colorectal cancer,²⁰ colon cancer^{9,41} and prostate cancer cells.¹¹ Recently, studies showed that DADS inhibited human colon cancer cell growth, invasion and migration, and reversed the EMT in gastric cancer cells⁴² and A549 lung cancer cells.¹⁰ MMP-2 and MMP-9 play a

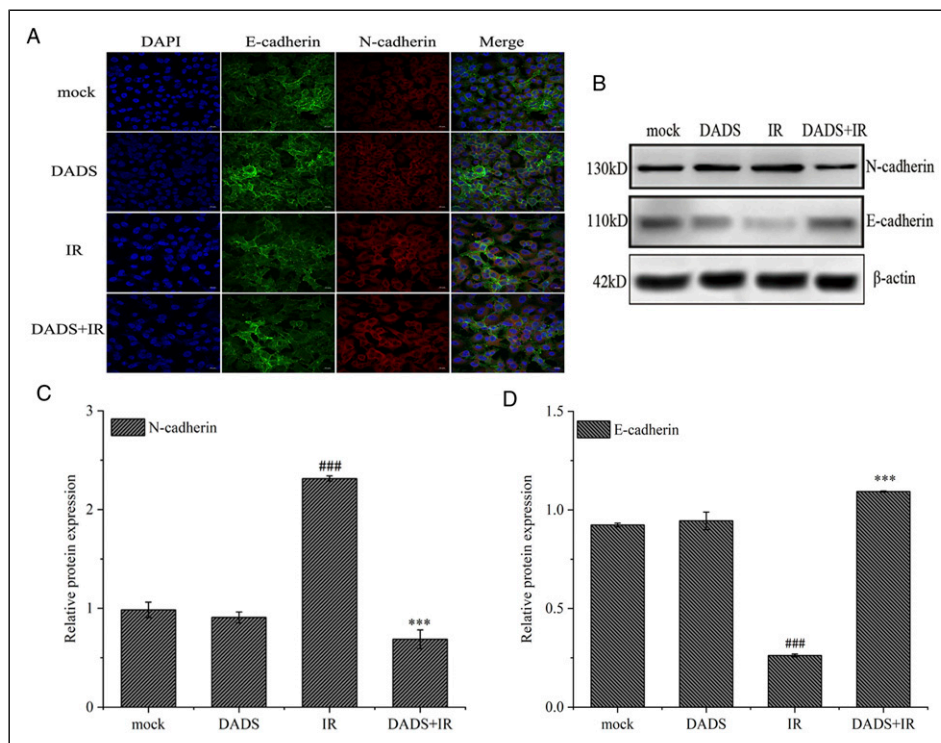


Figure 5. DADS suppressed IR-induced N-cadherin and E-cadherin expression in A549 cells. (A) Cells were treated with 40 μ M DADS or 4 Gy X-ray. After post-irradiation 24 h, the EMT markers, N-cadherin, and E-cadherin were analyzed by immunofluorescence (IF) staining. (scale bar, 20 μ m) (B-D) Western blotting was performed to determine the levels of N-cadherin and E-cadherin. ### $P < .001$ vs mock group; and *** $P < .001$ vs IR-treated group. Two-tailed Student's *t*-test. DADS: diallyl disulfide.

pivotal role in degrading the extracellular matrix, thus facilitating cell migration.⁴³⁻⁴⁵ A549 is one of the most aggressive lung cancer cell lines due to the aberrant expression of MMP-2 and MMP-9 expression.¹⁷ Furthermore, the cells are held together by tight junctions and adherent junctions, which are formed by cell surface epithelial cadherin (E-cadherin) molecules, whereas N-cadherin is associated with a more migratory and invasive phenotype; E-cadherin and N-cadherin are associated with more aggressive behavior of cell lines and tumors.⁴⁶ In this present study, our results also showed that pretreatment with 40 μ M DADS could enhance the radiosensitivity of A549 cells and attenuate IR-induced migration and invasion by inhibiting migration-related proteins MMP-2/9 expressions and suppressing IR-aggravated EMT marker. According to the current literature, its mechanisms of DADS action remain unclear, although it has been reported which included the suppression of DNA adduct formation, antioxidant activity, regulation of cell cycle arrest, induction of apoptosis and differentiation, histone modification, inhibition of angiogenesis and invasion, and so forth.

Numerous studies have shown that the deleterious effects of radiation include formation of free radicals and development of oxidative stress damage.⁴⁷ Nrf2 plays a pivotal role in endogenous protection in the defense against oxidative stress.²⁹ Indeed, several studies have shown that radiation activated the Nrf2 response and increased invasion and

metastasis of NSCLC.^{31,44,48} Our previous study also showed that IR induces the activation of Nrf2, knockdown of Nrf2 downregulated the expression of MMP-2, MMP-9, and N-cadherin, and suppressed IR-induced migration and invasion in A549 cells.³⁷ These findings implied that Nrf2 might participate in driving NSCLC invasion and metastasis. However, to date, little evidence is available on the effect of DADS on Nrf2 expression in A549 cells. Whether DADS inhibits IR-induced migration and invasion by regulating Nrf2 signaling pathway is still unknown. In the present study, we found that X-ray irradiation markedly aggravated Nrf2 and its regulated genes HO-1 and NQO1 mRNA and protein expression. Pretreatment with 40 μ M DADS significantly inhibited the levels of Nrf2 and its target genes HO-1 and NQO1 mRNA and protein expression in A549 cells. The results implied that Nrf2 was a target of DADS in the response of A549 cells to IR. Based on our previous results that knockdown of Nrf2 suppressed IR-induced migration and invasion in A549 cells, we speculated that DADS attenuated IR-induced migration and invasion of A549 cells by suppressing the activation of Nrf2 signaling.

Furthermore, Nrf2 dysregulation is implicated in lung cancer cell tumorigenicity and inhibited Nrf2 expression repressed tumor metastasis and invasion.^{26,27} Downregulation of Nrf2 inhibits osteopontin-induced migration.²⁸ In addition, inhibition of HO-1 and NQO1, the target genes of Nrf2, prevents the occurrence of metastasis.⁴⁹ In clinical practice, it

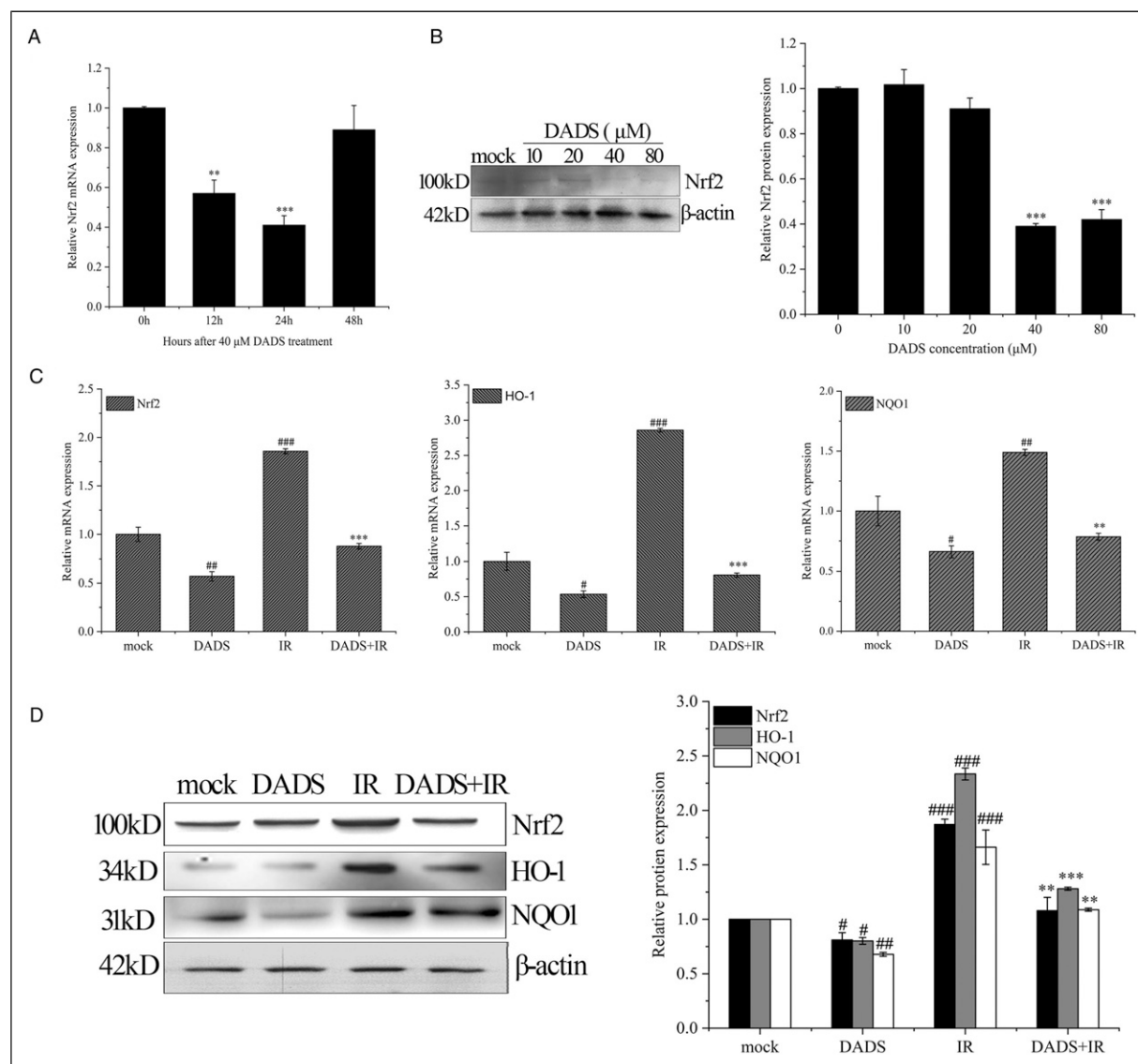


Figure 6. DADS inhibited IR-induced migration and invasion was associated with the suppression of Nrf2 signaling pathway. (A) Nrf2 mRNA levels were monitored by quantitative RT-PCR in A549 cells treated with 40 μM DADS for 12, 24, and 48 h. (B) Analysis of Nrf2 proteins by Western blotting in A549 cells treated with 40 μM DADS for 24 h. β-actin served as normalization control. (C) Expression of Nrf2, HO-1, and NQO1 mRNA was detected by RT-qPCR in A549 cells treated with 40 μM DADS and/or 4 Gy X-ray. (D) Western blotting analysis of Nrf2, HO-1, and NQO1 protein in A549 cells treated with 40 μM DADS and/or 4 Gy X-ray. ## $P < .05$, ### $P < .01$ and #### $P < .001$ vs mock group; * $P < .05$, ** $P < .01$, *** $P < .001$ vs IR-treated group; two-tailed Student's *t*-test. DADS: diallyl disulfide.

has been verified that Nrf2 and its target genes are overexpressed in NSCLC patients, giving cancer cells an advantage for survival and progression.^{50,51} Nrf2 expression was constitutively activated due to insertion and deletion mutations in Keap1 in some advanced NSCLC patients.³⁵ Nrf2 is thought to be responsible for NSCLC invasion and metastasis.⁴⁸ Thus, inhibition of Nrf2 and its target genes overexpression is the key to prevent or reverse radiotherapy-induced tumor recurrence and metastasis in treatment for NSCLC. Since pretreatment with DADS can markedly inhibit Nrf2 and its target genes HO-1 and NQO1 mRNA and protein expression, it has great potential for use in the development of a novel anti-metastatic

drug alone or in combination with radiotherapy for the treatment of NSCLC patients.

Conclusion

In summary, we revealed that low-dose ionizing radiation (4 Gy X-ray irradiation) induced migration and invasion potential of A549 cells and pretreatment with 40 μM DADS attenuated IR-induced migration and invasive properties. To the best of our knowledge, this is the first report of DADS attenuating IR-induced NSCLC metastasis, which is associated with the suppression of the Nrf2 signaling pathway. These

findings show that DADS might act as a therapeutic agent in the inhibition of cancer progression alone or in combination with radiotherapy for the treatment of NSCLC patients. However, the study had the limitation of using a single lung cancer line, A549. Further studies will be required to clarify whether DADS could directly regulate the expression of Nrf2 and maybe there exist other factors that mediate this relationship.

Authors' Contributions

HZ and AM conceived and designed the study. SX, FH, MX, DT, and JL performed the experiments. QZ, LG, and JS performed the data analysis and interpretation. AM and SX wrote the manuscript.

Declaration of conflicting interests

The author(s) declared no potential conflicts of interest with respect to the research, authorship, and/or publication of this article.

Funding

The author(s) disclosed receipt of the following financial support for the research, authorship, and/or publication of this article: This work was supported by grants from the Ministry of Science and Technology National Key R&D project (2018YFE020524), the National Natural Science Foundation of China (12065001), Gansu Provincial Science and Technology Project (20YF3FA021), Innovation Fund of Colleges and Universities in Gansu Province (2020A-041), and Zhaoqing Science and Technology Innovation Guidance Project (201904031412).

ORCID iD

Shuai Xu  <https://orcid.org/0000-0002-2220-7243>

References

- Sung H, Ferlay J, Siegel RL, et al. Global cancer statistics 2020: GLOBOCAN estimates of incidence and mortality worldwide for 36 cancers in 185 countries. *CA A Cancer J Clin*. 2021;71(3):209-249. doi:10.3322/caac.21660.
- Stencel K, Chmielewska I, Milanowski J, Ramlau R. Non-small-cell lung cancer: new rare targets-new targeted therapies-state of the art and future directions. *Cancers*. 2021;13(8):1829. doi:10.3390/cancers13081829.
- Jumeau R, Vilotte F, Durham AD, Ozsahin EM. Current landscape of palliative radiotherapy for non-small-cell lung cancer. *Transl Lung Cancer Res*. 2019;8:S192-S201. doi:10.21037/tlcr.2019.08.10.
- Roy SF, Louie AV, Liberman M, Wong P, Bahig H. Pathologic response after modern radiotherapy for non-small cell lung cancer. *Transl Lung Cancer Res*. 2019;8:S124-S134. doi:10.21037/tlcr.2019.09.05.
- Nesbit EG, Leal TA, Kruser TJ. What is the role of radiotherapy for extensive-stage small cell lung cancer in the immunotherapy era? *Transl Lung Cancer Res*. 2019;8:S153-S162. doi:10.21037/tlcr.2019.05.01.
- Jha P. Avoidable global cancer deaths and total deaths from smoking. *Nat Rev Canc*. 2009;9(9):655-664. doi:10.1038/nrc2703.
- Huang J, Yang B, Xiang T, et al. Diallyl disulfide inhibits growth and metastatic potential of human triple-negative breast cancer cells through inactivation of the β -catenin signaling pathway. *Mol Nutr Food Res*. 2015;59(6):1063-1075. doi:10.1002/mnfr.201400668.
- Zhou Y, Su J, Shi L, Liao Q, Su Q. DADS downregulates the Rac1-ROCK1/PAK1-LIMK1-ADF/cofilin signaling pathway, inhibiting cell migration and invasion. *Oncol Rep*. 2013;29(2):605-612. doi:10.3892/or.2012.2168.
- Lai KC, Hsu SC, Kuo CL, et al. Diallyl sulfide, diallyl disulfide, and diallyl trisulfide inhibit migration and invasion in human colon cancer colo 205 cells through the inhibition of matrix metalloproteinase-2, -7, and -9 expressions. *Environ Toxicol*. 2013;28(9):479-488. doi:10.1002/tox.20737.
- Das B, Sinha D. Diallyl disulphide suppresses the canonical Wnt signaling pathway and reverses the fibronectin-induced epithelial mesenchymal transition of A549 lung cancer cells. *Food Funct*. 2019;10(1):191-202. doi:10.1039/c8fo00246k.
- Shin DY, Kim GY, Kim JI, et al. Anti-invasive activity of diallyl disulfide through tightening of tight junctions and inhibition of matrix metalloproteinase activities in LNCaP prostate cancer cells. *Toxicol In Vitro*. 2010;24(6):1569-1576. doi:10.1016/j.tiv.2010.06.014.
- De Green D, Barton GEM, Sandberg EN, et al. Anticancer potential of garlic and its bioactive constituents: a systematic and comprehensive review. *Semin Canc Biol*. 2021;73:219-264. doi:10.1016/j.semcancer.2020.11.020.
- Hong YS, Ham YA, Choi JH, Kim J. Effects of allyl sulfur compounds and garlic extract on the expression of Bcl-2, Bax, and p53 in non small cell lung cancer cell lines. *Exp Mol Med*. 2000;32(3):127-134. doi:10.1038/emmm.2000.22.
- Hui C, Jun W, Ya LN, Ming X. Effect of *Allium sativum* (garlic) diallyl disulfide (DADS) on human non-small cell lung carcinoma H1299 cells. *Trop Biomed*. 2008;25(1):37-45.
- Molina JR, Yang P, Cassivi SD, Schild SE, Adjei AA. Non-small cell lung cancer: epidemiology, risk factors, treatment, and survivorship. *Mayo Clin Proc*. 2008;83(5):584-594. doi:10.4065/83.5.584.
- Xiao D, He J. Epithelial mesenchymal transition and lung cancer. *J Thorac Dis*. 2010;2(3):154-159. doi:10.3978/j.issn.2072-1439.2010.02.03.7.
- Hwang KE, Kim HJ, Song IS, et al. Salinomycin suppresses TGF- β 1-induced EMT by down-regulating MMP-2 and MMP-9 via the AMPK/SIRT1 pathway in non-small cell lung cancer. *Int J Med Sci*. 2021;18(3):715-726. doi:10.7150/ijms.50080.
- Park J, Schwarzbauer JE. Mammary epithelial cell interactions with fibronectin stimulate epithelial-mesenchymal transition. *Oncogene*. 2014;33(13):1649-1657. doi:10.1038/onc.2013.118.
- Li CL, Yang D, Cao X, et al. Fibronectin induces epithelial-mesenchymal transition in human breast cancer MCF-7 cells via activation of calpain. *Oncol Lett*. 2017;13(5):3889-3895. doi:10.3892/ol.2017.5896.

20. Li J, Wu DM, Han R, et al. Low-dose radiation promotes invasion and migration of A549 cells by activating the CXCL1/NF- κ B signaling pathway. *OncoTargets Ther.* 2020;13:3619-3629. doi:10.2147/ott.s243914.
21. Vilalta M, Rafat M, Graves EE. Effects of radiation on metastasis and tumor cell migration. *Cell Mol Life Sci.* 2016;73(16):2999-3007. doi:10.1007/s00018-016-2210-5.
22. Blyth BJ, Cole AJ, MacManus MP, Martin OA. Radiation therapy-induced metastasis: radiobiology and clinical implications. *Clin Exp Metastasis.* 2018;35(4):223-236. doi:10.1007/s10585-017-9867-5.
23. Di C, Sun C, Li H, et al. Diallyl disulfide enhances carbon ion beams-induced apoptotic cell death in cervical cancer cells through regulating Tap73/ Δ Np73. *Cell Cycle.* 2015;14(23):3725-3733. doi:10.1080/15384101.2015.1104438.
24. Gañán-Gómez I, Wei Y, Yang H, Boyano-Adánez MC, García-Manero G. Oncogenic functions of the transcription factor Nrf2. *Free Radic Biol Med.* 2013;65:750-764. doi:10.1016/j.freeradbiomed.2013.06.041.
25. Satoh H, Moriguchi T, Taguchi K, et al. Nrf2-deficiency creates a responsive microenvironment for metastasis to the lung. *Carcinogenesis.* 2010;31(10):1833-1843. doi:10.1093/carcin/bgq105.
26. Singh A, Boldin-Adamsky S, Thimmulappa RK, et al. RNAi-mediated silencing of nuclear factor erythroid-2-related factor 2 gene expression in non-small cell lung cancer inhibits tumor growth and increases efficacy of chemotherapy. *Canc Res.* 2008;68(19):7975-7984. doi:10.1158/0008-5472.can-08-1401.
27. DeNicola GM, Karreth FA, Humpton TJ, et al. Oncogene-induced Nrf2 transcription promotes ROS detoxification and tumorigenesis. *Nature.* 2011;475(7354):106-109. doi:10.1038/nature10189.
28. Lu DY, Yeh WL, Huang SM, Tang CH, Lin HY, Chou SJ. Osteopontin increases heme oxygenase-1 expression and subsequently induces cell migration and invasion in glioma cells. *Neuro Oncol.* 2012;14(11):1367-1378. doi:10.1093/neuonc/nos262.
29. Wang H, Liu X, Long M, et al. NRF2 activation by antioxidant antidiabetic agents accelerates tumor metastasis. *Sci Transl Med.* 2016;8(334):334ra51. doi:10.1126/scitranslmed.aad6095.
30. Zhang L, Wang N, Zhou S, Ye W, Jing G, Zhang M. Propofol induces proliferation and invasion of gallbladder cancer cells through activation of Nrf2. *J Exp Clin Canc Res.* 2012;31:66. doi:10.1186/1756-9966-31-66.
31. Wang J, Konishi T. Nuclear factor (erythroid-derived 2)-like 2 antioxidative response mitigates cytoplasmic radiation-induced DNA double-strand breaks. *Canc Sci.* 2019;110(2):686-696. doi:10.1111/cas.13916.
32. Zhao Q, Mao A, Yan J, et al. Downregulation of Nrf2 promotes radiation-induced apoptosis through Nrf2 mediated Notch signaling in non-small cell lung cancer cells. *Int J Oncol.* 2016;48(2):765-773. doi:10.3892/ijo.2015.3301.
33. Aljohani HM, Aittaleb M, Furgason JM, et al. Genetic mutations associated with lung cancer metastasis to the brain. *Mutagenesis.* 2018;33(2):137-145. doi:10.1093/mutage/gey003.
34. Sitthideatphaiboon P, Galan-Cobo A, Negro MV, et al. STK11/LKB1 mutations in NSCLC are associated with KEAP1/NRF2-dependent radiotherapy resistance targetable by glutaminase inhibition. *Clin Canc Res.* 2020;27:1720-1733. doi:10.1158/1078-0432.ccr-20-2859.
35. Singh A, Misra V, Thimmulappa RK, et al. Dysfunctional KEAP1-NRF2 interaction in non-small-cell lung cancer. *PLoS Med.* 2006;3(10):e420. doi:10.1371/journal.pmed.0030420.
36. Tong YH, Zhang B, Yan YY, et al. Dual-negative expression of Nrf2 and NQO1 predicts superior outcomes in patients with non-small cell lung cancer. *Oncotarget.* 2017;8(28):45750-45758. doi:10.18632/oncotarget.17403.
37. Zhao Q, Mao A, Guo R, et al. Suppression of radiation-induced migration of non-small cell lung cancer through inhibition of Nrf2-Notch axis. *Oncotarget.* 2017;8(22):36603-36613. doi:10.18632/oncotarget.16622.
38. Bray F, Ferlay J, Soerjomataram I, Siegel RL, Torre LA, Jemal A. Global cancer statistics 2018: GLOBOCAN estimates of incidence and mortality worldwide for 36 cancers in 185 countries. *Ca - Cancer J Clin.* 2018;68(6):394-424. doi:10.3322/caac.21492.
39. Perlikos F, Harrington KJ, Syrigos KN. Key molecular mechanisms in lung cancer invasion and metastasis: a comprehensive review. *Crit Rev Oncol Hematol.* 2013;87(1):1-11. doi:10.1016/j.critrevonc.2012.12.007.
40. Su B, Su J, He H, et al. Identification of potential targets for diallyl disulfide in human gastric cancer MGC-803 cells using proteomics approaches. *Oncol Rep.* 2015;33(5):2484-2494. doi:10.3892/or.2015.3859.
41. Su J, Zhou Y, Pan Z, et al. Downregulation of LIMK1-ADF/cofilin by DADS inhibits the migration and invasion of colon cancer. *Sci Rep.* 2017;7:45624. doi:10.1038/srep45624.
42. Su B, Su J, Zeng Y, et al. Diallyl disulfide suppresses epithelial-mesenchymal transition, invasion and proliferation by down-regulation of LIMK1 in gastric cancer. *Oncotarget.* 2016;7(9):10498-10512. doi:10.18632/oncotarget.7252.
43. Qian Q, Wang Q, Zhan P, et al. The role of matrix metalloproteinase 2 on the survival of patients with non-small cell lung cancer: a systematic review with meta-analysis. *Canc Invest.* 2010;28(6):661-669. doi:10.3109/07357901003735634.
44. Sielens W, Polzer B, Elshawi K, et al. Cellular localization of EMMPRIN predicts prognosis of patients with operable lung adenocarcinoma independent from MMP-2 and MMP-9. *Mod Pathol.* 2008;21(9):1130-1138. doi:10.1038/modpathol.2008.102.
45. Halbersztadt A, Haloń A, Pajak J, Robaczyński J, Rabczynski J, St Gabryś M. [The role of matrix metalloproteinases in tumor invasion and metastasis]. *Ginek Pol.* 2006;77(1):63-71.
46. Dongre A, Weinberg RA. New insights into the mechanisms of epithelial-mesenchymal transition and implications for cancer. *Nat Rev Mol Cell Biol.* 2019;20(2):69-84. doi:10.1038/s41580-018-0080-4.
47. Tharmalingam S, Sreetharan S, Kulesza AV, Boreham DR, Tai TC. Low-dose ionizing radiation exposure, oxidative stress and epigenetic programming of health and disease. *Radiat Res.* 2017;188(4):525-538. doi:10.1667/rr14587.1.

48. Ohta T, Iijima K, Miyamoto M, et al. Loss of Keap1 function activates Nrf2 and provides advantages for lung cancer cell growth. *Canc Res.* 2008;68(5):1303-1309. doi:[10.1158/0008-5472.can-07-5003](https://doi.org/10.1158/0008-5472.can-07-5003).
49. Ishikawa T, Yoshida N, Higashihara H, et al. Different effects of constitutive nitric oxide synthase and heme oxygenase on pulmonary or liver metastasis of colon cancer in mice. *Clin Exp Metastasis.* 2003;20(5):445-450. doi:[10.1023/a:1025448403124](https://doi.org/10.1023/a:1025448403124).
50. Hayes JD, McMahon M. NRF2 and KEAP1 mutations: permanent activation of an adaptive response in cancer. *Trends Biochem Sci.* 2009;34(4):176-188. doi:[10.1016/j.tibs.2008.12.008](https://doi.org/10.1016/j.tibs.2008.12.008).
51. Kikuchi A, Yamaya M, Suzuki S, et al. Association of susceptibility to the development of lung adenocarcinoma with the heme oxygenase-1 gene promoter polymorphism. *Hum Genet.* 2005;116(5):354-360. doi:[10.1007/s00439-004-1162-2](https://doi.org/10.1007/s00439-004-1162-2).